

## SiC-Based Magnetic-less DC-DC Converter with Wide Temperature Range Operation

**Abstract:** This paper presents a concept and experimental results of the magnetic-less converter suitable for wide temperature range operation. The DC-DC converter uses a variant of a switched-capacitor voltage multiplier topology, silicon carbide (SiC) and IGBT (insulated gate bipolar transistor) semiconductors and resonant circuits with air-based chokes designed on PCB (printed circuit board), as well as high temperature resonant capacitors and PCB materials. Ferrite materials are not required which and therefore the problems with inductance variation versus temperature do not exist.

**Streszczenie.** W artykule przedstawiono koncepcję i wyniki doświadczalne przekształtnika do pracy w szerokim zakresie temperatur. W przekształtniku zastosowano wariant topologii rezonansowo przełączalnych kondensatorów, półprzewodniki z węgla krzemu (SiC) i IGBT oraz obwody rezonansowe z dławikami powietrznymi zaprojektowanymi na PCB, a także wysokotemperaturowe kondensatory rezonansowe oraz specjalny materiał PCB. Rdzeń ferrytowy nie został tu zastosowany, a zatem nie istnieje problemy ze zmianą indukcyjności w zależności od temperatury pracy układu. (**Przekształtnik DC-DC bazujący na SiC pracujący w szerokim zakresie temperatur**).

**Keywords:** Switched capacitor voltage converter; High temperature power converter; Zero current switching; DC-DC converter.

**Słowa kluczowe:** Przełączalne kondensatory, Praca układu w wysokiej temperaturze, przełączanie w zerze prądu, Przekształtnik DC-DC.

### Introduction

The development of power electronic converters towards high temperature of operation is one of the important trend owing to an increase of junction temperature of semiconductor switches. Silicon carbide semiconductors can operate at temperatures junction temperature above 500°C [1], while the silicon limits are around 200°C. Examples of applications can be the oil drilling industry, space exploration, aviation and the automotive industry [1] and [2]. The high-temperature converter should be assigned to a particular application category even at the design stage because the temperature differences are significant. However, the failure mechanisms of SiC MOSFETs (Metal-Oxide Semiconductor Field-Effect Transistor) can be easily generated by current or high-temperature-related gate oxide damage [3]. Beside of MOSFET SiC transistor, the possible solution in the future industry application is to the hybrid switch: SI IGBT with SiC MOSFET. The hybrid switch can achieve operation in high-temperature with high current stress [4]. In [5] SiC transistors were used, to develop a converter that would allow continuous working at 320°C (junction temperature) and gives opportunities for the application of the system in the drilling industry as well as in the automotive or aerospace industries. The proposed system in [5] allowed to work for 80 hours at a temperature of 470 Celsius degrees (junction temperature). Presented results [4], [5] for the high-temperature SiC operation (above 180°C) have been obtained in a laboratory setup. The temperature of the commercially available switches would be limited by the package of the transistors. In [6], the developed circuits are classic Three-Phase AC-DC Inverter, which operating temperature of both gate driver and power circuit is targeted at 180 °C. SiC technology is also introduced to traction inverters with liquid cooling system [7] and [8]. An example of SiC parameters for electric vehicles (EV) and their characterization can be found in [9] and for the high voltage application (3.3 kV / 400 A) SiC transistors [10]. SiC-CMOS digital circuits are also thematically current research and prototypes reach operating temperatures up to 400 degrees [11].

Aside from the application of appropriate semiconductor switch the high temperature power electronic converter requires suitable topology, passive components and mechanical materials. Selection of a topology of a converter

where ferrite-based chokes are not required is a great merit in high temperature design. In the field of DC-DC converters the topologies based-on switched-capacitor (SC) technology can be adequate. In the SC converter [12] the majority of energy is transferred via a capacitor. Inductors are used as low energy resonant components and can be achieved as an air-based choke. The converter presented in this paper bases on the SC technique of energy conversion [13]-[20] in the topology of a Cost-Effective Resonant Switched Capacitor Voltage Multiplier (SCVM) presented in [16]. This is a high voltage gain converter which can multiply voltage  $N$  times (where  $N$  is the number of cells). The switching capacitors converters family is significant and the SC converters can be designed not only in configuration step-up [14]-[18] but also as step-down topologies [20].

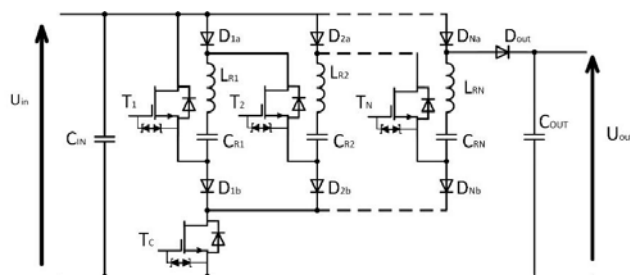


Fig. 1. Cost-Effective Resonant Switched Capacitor Voltage Multiplier (CESCVM). General concept with  $N$  switching cells and JFET transistors.

The CESCVM topology of the designed converter is presented in Fig. 1. Such converter contains a fewer number of transistors in comparison to the basic SCVM [14] and [15]. In the [16] feasibility of the CESCVM is demonstrated with the utilization of silicon MOSFET switches with  $V_{DSmax} = 175$  V. However the voltage stress on  $T_C$  transistor can reach the level of the output voltage. Therefore, to design the converter for higher voltage the switches for higher voltages are required.. SiC switches achieves significantly lower FOM (figure of merit expressed as  $nC \cdot m\Omega$ ) than high voltage Si switches. Parameters of switches applied in the CESCVM are critical for operation of the converter. The topology of CESCVM is established but he research concepts and results related to high voltage,

high temperature, high efficiency and low volume of CESCVM are aspects which are novel in this paper. The proposed design concept of the CESCVM assumes the use of SiC JFETs (Junction Field-Effect Transistor) transistors and operation with the temperature of the case of that reaches 150°C ( $T_j$  between 150°C and 175°C). Application of SiC switches changes the design in relation to Si low voltage Mosfets do to the following parameters: switching losses associated with  $C_{oss}$  and VCE versus switching frequency, conduction losses versus temperature. Variation of  $R_{ds(on)}$  resistance versus the junction temperature can be critical in the converter for high temperature operation. In the case of SiC – based design the variation is adequately low which is confirmed by efficiency results in this paper. Similarly, the results of the CESCVM efficiency versus the switching frequency demonstrates low impact of  $C_{oss}$  losses in the case of operation with 100V/400V conversion ratio. Such issues are not presented in [16] however the SiC-based CESCVM demonstrate its adequate parameters for high voltage and high temperature design.

Other novel aspects relates to high overall temperature design and operation of the CESCVM converter. In the analyzed design, semiconductors are placed on a PCB board directly and therefore the PCB material, as well as capacitors, are selected as high temperature components. An increase of the temperature of the converter makes it possible to decrease the heat sink volume and finally to increase the power density. Furthermore, because the CESCVM converter may operate with air-based resonant chokes or with parasitic inductances, the design towards the high temperature operation can be favorable for various applications. In such a design the converter could operate in high ambient temperature as well. The gate driver system is separated from the main circuit by air distances and is not heated by the power transistors and diodes. For the proposed converter an impact of frequency and load of the converter on the efficiency and voltage gain at a high-temperature is investigated.

The range of temperature of transistors achieved in the tests enables a comparison of the SiC and IGBT-based parameters of the CESCVM which is novel research as well. For both the cases characteristics of efficiency versus the output power are presented and compared. The performed results demonstrate the feasibility of the IGBT-based CESCVM and acceptable results of efficiency. The IGBT-based solution of the CESCVM achieved lower efficiency in comparison to SiC-based. However the difference in efficiency results is not very significant and IGBT-based CESCVM can be an attractive low-cost approach.

The design concept for the high-temperature converter, presented in this paper, may be useful for the automotive industry [9], [10] and other SC converters such as SCVM-based [13]-[20].

The paper is organized as follows. Section 2 presents an analytical description of the converter. Section 3 describes in detail the structure of the CESCVM DC-DC converter. Application of suitable PCB material [21] as well as capacitors selected for high temperature operation [22]-[24], makes it possible to implement SC converter to operate with high temperatures. The test setup and results of experiments are presented in Section 4. The last part of the article consists of major conclusions.

### Principle of operation of the converter

The CESCVM converter works in two cycles in each switching period. In the first one, switched capacitors are charging from the input source by means of  $T_C$  switch. Fig. 2 and Fig. 3 presents the general concept of charging and

discharging the switched capacitors for three cell topology of CESCVM. In the second cycle of operation, the capacitors are discharging by means of  $T_1$ ,  $T_2$  and  $T_3$ . Air chokes can be used in converters to achieve a resonant converter with ZCS (zero current switching) [12]. Assuming constant value of input and output voltage, the capacitor charging current can be described by the equation (current response of series RLC circuit):

$$(1) i_{Cn}(t) = e^{\alpha_{(1)}t} \frac{U_{IN} - U_{Cmin}}{\omega_{(1)}L_{\Sigma(1)}} \sin(\omega_{(1)}t),$$

and the angular resonant frequency for first stage:

$$(2) \omega_{(1)} = \sqrt{\frac{1}{C \cdot L_{\Sigma(1)}} + \alpha_{(1)}},$$

where:  $U_{IN}$  - is the input voltage,  $U_{Cmin}$  - is the minimum voltage across capacitors  $C = C_{R1} = C_{R2} = C_{R3}$  (assuming identical capacitors in the converter circuit),  $L_{\Sigma(1)}$  - is the summarized inductance of circuits during the charging stage (air choke inductance and parasitic inductance of the PCB signal traces),  $\alpha_{(1)}$  - is the damping factor:

$$(3) \alpha_{(1)} = -\frac{R_{S(1)}}{2L_{\Sigma(1)}},$$

where:  $R_{S(1)}$  is the resistance of the circuit during the charging process including transistor  $T_C$

This resistance can be calculated by the sum of ESR value, the choke resistance and the turn-on resistance of the switch. The resistance of the circuit during the charging process is not significant, which simplifies equation (1) and (2) to the following:

$$(4) i_{Cn}(t) = \frac{U_{IN} - U_{Cmin}}{\omega_{(1)}L_{\Sigma(1)}} \sin(\omega_{(1)}t),$$

$$(5) \omega_{(1)} = \sqrt{\frac{1}{C \cdot L_{\Sigma(1)}}},$$

The total resistance of the resonant circuits is composed of the choke resistance, the ESR value of the capacitor,  $R_{DS(on)}$  and the parasitic resistance of the PCB signal traces. In the second step of operation, the switched capacitors are discharged to the output capacitor by means of switch  $T_1$ ,  $T_2$  and  $T_3$ . In this stage, the current can be described by the following formula:

$$(6) i_C(t) = e^{\alpha_{(2)}t} \frac{U_{IN} - U_{OUT} + N \cdot U_{Cmax}}{\omega_{(2)} \cdot L_{\Sigma(2)}} \sin(\omega_{(2)}t),$$

and the angular resonant frequency for second stage is the following:

$$(7) \omega_{(2)} = \sqrt{\frac{1}{C \cdot L_{\Sigma(2)}} + \alpha_{(2)}},$$

and the damping factor will change to:

$$(8) \alpha_{(2)} = -\frac{R_{S(2)}}{2L_{\Sigma(2)}},$$

where:  $U_{OUT}$  - is the output voltage,  $U_{Cmax}$  - is the maximum voltage across capacitors,  $L_{\Sigma(2)}$  - is the summarized inductance of the circuit during the discharging stage,  $R_{S(2)}$  - is the resistance of the circuit during the discharging stage.

And the simplification of the (6) and (7) without damping factor  $\alpha_{(2)}$ :

$$(9) i_{T1}(t) = \frac{U_{IN} - U_{OUT} + N \cdot U_{Cmax}}{\omega_{(2)} \cdot L_{\Sigma(2)}} \sin(\omega_{(2)}t),$$

and the angular resonant frequency:

$$(10) \omega_{(2)} = \sqrt{\frac{1}{C \cdot L_{\Sigma(2)}}}$$

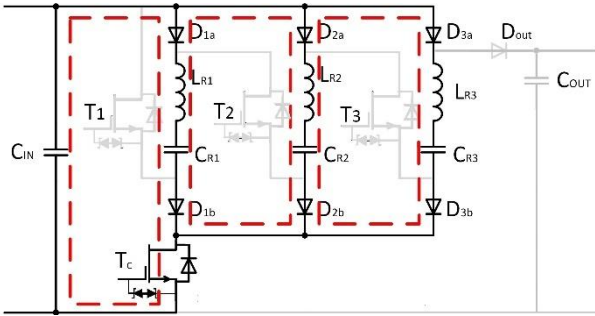


Fig. 2. CESCVM operation for topologies with  $N = 3$ . Charging capacitors of all resonant cells,

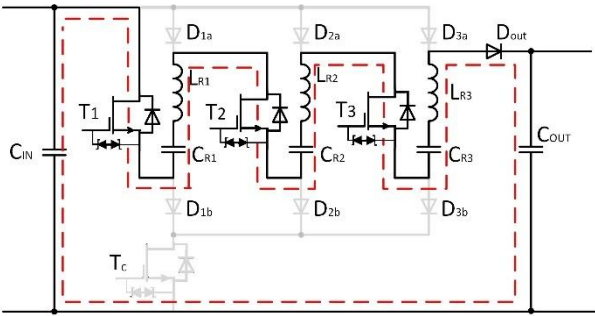


Fig. 3. CESCVM operation for topologies with  $N = 3$ . Discharging the switched capacitors and charging the output capacitor.

The voltage of the capacitors during charging are (no damping factor):

$$(11) \quad u_{CI}(t) = U_{IN} + (U_{Cmin} - U_{IN})\cos(\omega_{(1)}t),$$

And voltage during discharging process:

$$(12) \quad u_{CII}(t) = \frac{U_{OUT} - U_{IN}}{n} + (U_{Cmax} - \frac{U_{OUT} - U_{IN}}{n})\cos(\omega_{(2)}t),$$

The theoretical output voltage of the idealized  $N$  cells CESCVM converter depends only on the number of switching cells and can be described as:

$$(13) \quad U_{OUT} = (1 + N) \cdot U_{IN},$$

where:  $U_{IN}$  is the input voltage,  $N$  is the number of cells with switched capacitors.

One of the important features of the converter is different voltage stress on semiconductor switches. The voltage on discharge transistors  $T_1$ ,  $T_2$  and  $T_3$  is the same and varies from  $U_{IN}$  to  $2U_{IN}$ . The voltage on the diodes increases respectively 1, 2 and 3 times in relation to  $U_{IN}$ . The charging currents of the resonant capacitors are summed and flow through the  $T_C$  transistor. Consequently, the  $T_C$  transistor conducts threefold larger current than others and has the highest drain-source voltage, which equals to the output voltage ( $U_{OUT}$ ). Therefore the switching losses and  $C_{oss}$  losses of  $T_C$  transistor are supposed to be significant.

Diodes  $D_{1b}-D_{nb}$  blocks the unrequired oscillatory current flow in  $LC$  branches short circuit when the transistors  $T_1$  and  $T_2$  are in the on-state (as in the stage of discharging presented in Fig. 2 (b)). The same function is complied with by  $D_{1a}-D_{na}$  diodes.

### Design Concept of main power circuit

The design concept assumes demonstration of the DC-DC converter operating in increased temperature which can occur due to high temperature increment in low volume design or high ambient temperature. It is assumed that all the components in the power section will not exceed 150 degrees. Fig. 4 presents the concept of the experimental setup of the converter assembled on PCB. The design is composed of two main parts where the power components are located on a board area with a high temperature of operation. The second part contains gate drivers and is placed on the part of the PCB separated from the warm components by air distance (Fig. 3). The heat is generated in the power section mostly and the part with gate drivers operates at a significantly lower temperature.

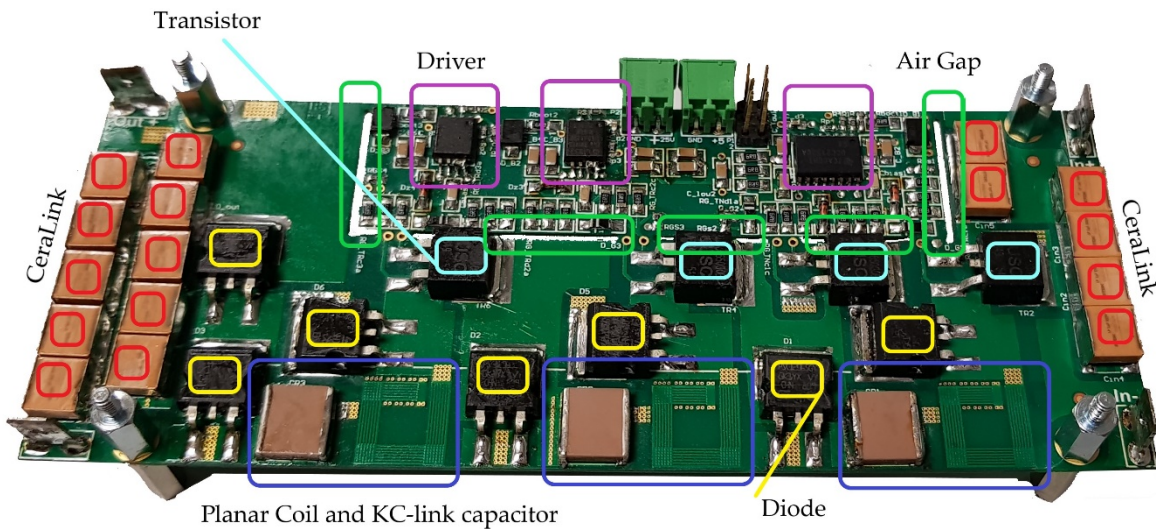


Fig. 4. The experimental model of CESCVM converter for high temperature operation and a detailed described circuit.

The proposed CESCVM design is created with the use of the PCB board composed with SH260 laminate. It is the high performance and high glass transition temperature, which exceeds  $T_g > 250^\circ\text{C}$ . Decomposition temperature  $T_d$  is over  $417^\circ\text{C}$  [21]. The power system consists of a 6-layer PCB system. The CESCVM is a converter operating

according to the switched capacitor concept. The vast majority of energy is transferred via capacitors. Low inductance chokes are used for ZCS operation which occurs by oscillations of currents. High temperature has a negative impact on the ferrite-core chokes parameters by the decrease of saturation magnetic flux density [22].

However, in the proposed design, the suitable resonant circuits operation is achieved with the use of PCB air-based chokes. The inductance value of the designed chokes is equal to 0,32  $\mu\text{H}$  and has been accomplished on 6 turns coil created on 6 layers. In the adequate temperature range higher resonant inductances and lower EMI intensity can be achieved with the use of a ferrite-core choke composed of materials suitable for wide temperature range such as 3C95. The width of the windings of chokes are designed sufficiently high to minimize stray resistance (Fig. 3). Air-core based design force the flux is in the air which couples with associated components with the power circuits especially sensors and gate drives. To avoid coupling in the power board, air-chokes must be placed as far as possible from all integrated circuits.

In the proposed design, two types of capacitors are used, namely CeraLink [23] in input and output banks and KC-Link type [24] as switched capacitances. Both types of capacitors have an adequate allowable operating temperature. In the proposed design, the temperature of capacitors is lower than the hot spot in the vicinity of transistors where losses generation is the highest. The resonance capacitance is equal to 0,66  $\mu\text{F}$  for each cell. The values of inductance and capacitance have been determined using the HM8118 LCR Bridge device for frequency 100 kHz and in the temperature equal to 20°C. The calculated resonance frequency ( $f_r$ ) of the system is correspondingly 346,32 kHz. The converter operates in zero current switching mode with switching frequency below the resonant frequency  $f_s < f_r$ .

In the presented design, it is assumed that the transistors operates with junction temperature above 150°C (150°C to 175°C). The tested transistors belong to families with  $T_j = 175^\circ\text{C}$ . From the former research results [15], [16] it is known that, from the efficiency standpoint, the most important parameters of transistor selected to SCVM-type converters are low  $R_{DS(on)}$  and low  $C_{oss}$ . The figure of merit for the proposed design should be composed with these two parameters. Due to high voltage stress on  $T_4$  switch and increased operating temperature SiC switches have been taken into consideration.

The selected transistor for tests is SiC JFETs UJ3C065030B3 with a cascode optimized MOSFET. Its  $R_{DS(on)}$  is 43 m $\Omega$  for 175°C,  $C_{oss}$  is 320 pF [25]. Low gate charge assures low heat generation in the driver part of PCB. The transistor is in the SMD case and will be assembled on the PCB board as  $T_1 - T_C$  (Fig. 2. Fig. 3.). In the former research results of the SCVM converter, reported in [14] low voltage 150 V MOSFET was using, where  $C_{oss}$  is 327 pF, total gate charge 31.3 pF (to 47 pF) and  $R_{DS(on)} = 14 - 23 \text{ m}\Omega$ .

To compare the SiC-based performance with Si-based, the IGBT transistor has been selected for tests of the converter (IKB15N65EH5 - high speed switching series 5th generation, with the output capacitance  $C_{oss} = 24 \text{ pF}$ , and  $V_{CESat} = 1,95 \text{ V}$  at 175°C [26]). Switching times of this component are adequate for the operational conditions in the proposed design of CESCVM. Application of this switch in the should result in very low switching turn-on losses due to low output capacitance.

The SiC diodes STPSC1206 with 650 V  $V_{RRM}$  and with the same maximum operating temperature as the transistors  $T_{jmax} = 175^\circ\text{C}$  have been used in the design.

### Design Concept of the gate driver

To make the design flexible, for the tests with SiC, IGBT as well as JFET or MOSFET transistors the gate driver with negative voltage allowable to turn off the transistor is used. It is very important that the entire converter uses only one

supply source for gate drivers operation by the application of a bootstrap supply circuit. However, the proposed solution makes it possible to achieve a negative voltage of low-side ( $T_C$ ) and high-side ( $T_1 - T_3$ ) transistors. Fig. 5 depicts an isolated dual-channel gate driver UCC21520. It is an obligatory condition to provide thermal isolation for the driver circuit. In the presented circuit 1,5 mm space was designed to prevent the high temperature transfer from high voltage power circuit to a low voltage driver (Fig. 4).

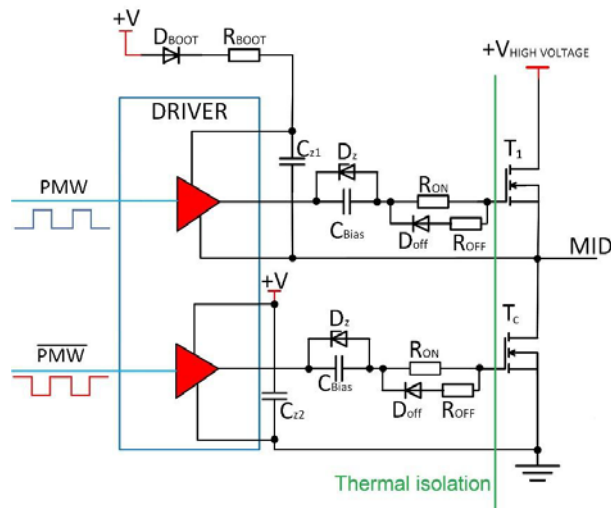


Fig. 5. The applied concept of the bootstrap circuit with capacitor and antiparallel Zener diode in transistor gate circuit. Thermal insulation is made by the air gap on the PCB.

The negative gate driver voltage is achieved by using a capacitor and an antiparallel Zener diode in the gate circuit [27]. The value of the negative gate drive bias is not only determined by the Zener diode. Negative voltage can also change when the duty cycle changes but the proposed topology have a fixed duty cycle (equal to 50%). Gate-source voltage and current for an operating transistor are shown in the Fig. 5.

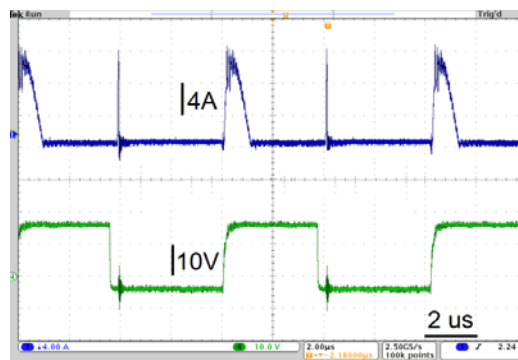


Fig. 6. The Current and the gate-source voltage of the high-side transistor. Switching frequency:  $f_s = 125 \text{ kHz}$ .

### Experimental Results

Fig. 7. presents the experimental waveforms of the transistors current, input and output voltage of the CESCVM (Fig. 2 and Fig. 3.). The results confirm the feasibility of the converter and its operating idea ( $f_s = 150 \text{ kHz}$ ,  $U_{in} = 100\text{V}$ ). The converter operation is consistent with the theoretical and simulation predictions. The CESCVM converter in the proposed design has been tested to determine efficiency and voltage gain as well.

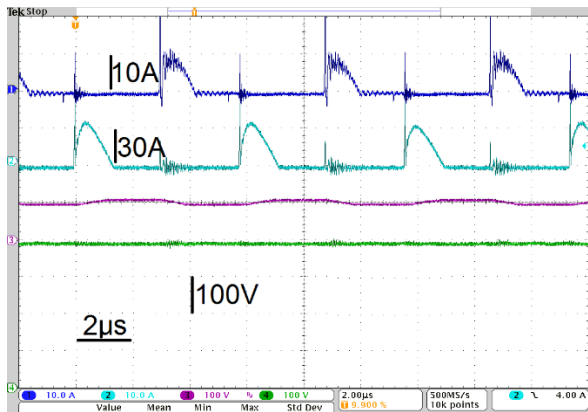


Fig. 7. Experimental waveforms of the transistors current, input and output voltage of the CESCVM. CH1 - T1 high-side transistor drain current, CH2 – TC low-side transistor drain current, CH3 - input voltage and CH4 - output voltage of the CESVM.

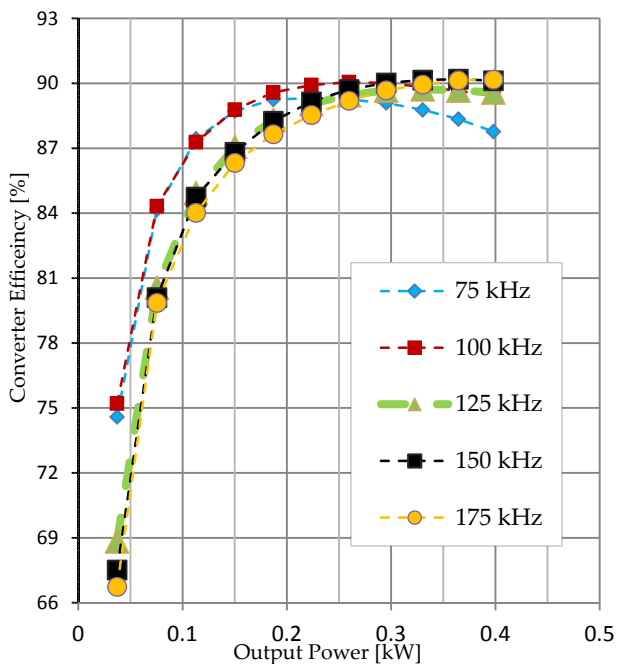


Fig. 8. Experimental results of the converter at the case temperature 150°C: (a) efficiency vs. output power., (b) efficiency vs. switching frequency at  $P_{out}=400$  Watt.

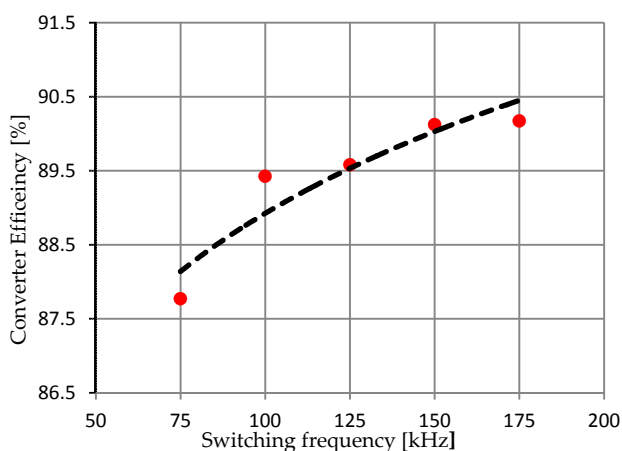


Fig. 9. Experimental results of the converter at the case temperature 150°C: (a) efficiency vs. output power., (b) efficiency vs. switching frequency at  $P_{out}=400$  Watt.

A series of measurements have been performed for the designed converter for various switching frequency values (Fig. 7 and Tab. 1). The efficiency was precisely measured with the use of Yokogawa WT 1500 Power Meter. Based on Fig. 7. the highest value of efficiency is equal to 90,21% and occurs at  $P_{OUT} \approx 360$  W and frequency equal to 150 kHz. The efficiency of the converter is relatively low and it is caused by inconvenient switching conditions for charging transistor. The Volumetric Power Density of the converter is equal to 7,12 kW/dm<sup>3</sup> for the highest tested output power (400 W).

With lower switching frequency the conduction losses will be higher due to time intervals between the current pulses. Charging and discharging of the switched capacitors should be minimized to achieve higher efficiency of the classic SCVM or proposed CESCVM. Shortened the time interval can be minimized by an increase in switching frequency. However, it will increase switching losses, which shows Fig. 8 and Table 1 where efficiency does not change drastically. The efficiency peak value only occurs for a different power value, which should be introduced during the designing process. Based results from Fig. 9. the CESCVM for high power application require increased frequency to achieve maximum efficiency.

Table. 1. Peak of the converter efficiency vs. transistor switching frequency.

Frequency [kHz]	Peak efficiency [%]
75	89,32
100	90,06
125	89,73
150	90,20
175	90,15

In the presented results the converter switching frequency is above 150 kHz and it is difficult to meet EMI specifications for power supplies standard. Electromagnetic standards may change in the future and the frequency above 150 kHz will be allowed in practice [27].

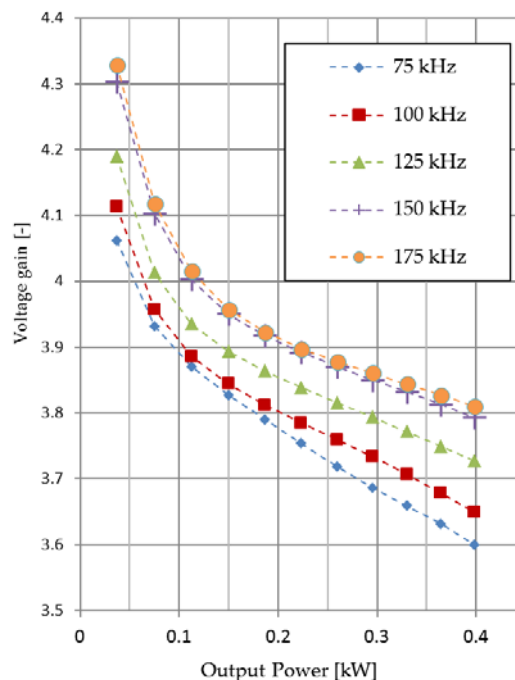


Fig. 10. Experimental results of the converter at the case temperature 150°C - voltage gain vs. output power at  $P_{out} = 400$  Watts.

The measured voltage gain of the converter is presented in Fig. 10. The measurements have been performed for various values of switching frequency and a fixed duty ratio (50%). The voltage gain for bigger load value is lower than the theoretical value  $GU = 4,0$  ( $U_{IN} = 100$  V and  $U_{out} = 400$  V). An interesting fact is that the voltage gain does not change linearly versus the output power and a rapid drop in low power region (below 100 W) is visible and then the gain starts to decrease linearly. The increment of switching frequency can provide higher voltage gain value for high output power (Fig. 11.).

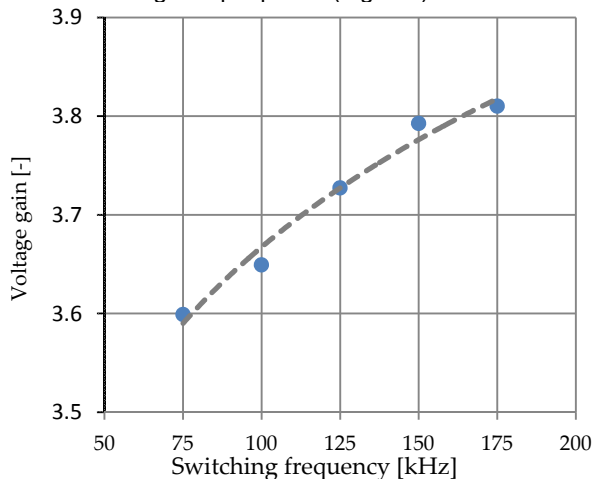


Fig. 11. Experimental results of the converter at the case temperature 150°C - voltage gain vs. switching frequency at  $P_{out}=400$  Watts.

#### Experimental Results for IGBT-based CESCVM

To prove the correctness of the SiC transistors application for high temperature CESCVM, the power circuit was redesigned to perform the tests with silicon 5th generation IGBT switches IKB15N65EH5-DS-v02. The basic parameters of this switch are presented in Section 3.2 and [26]. Fig. 12. presents the experimental waveforms of the IGBT transistor current, capacitor voltage, input and output voltage of the CESCVM with IGBTs and Fig. 9. the chart of the voltage gain and efficiency versus the output power.

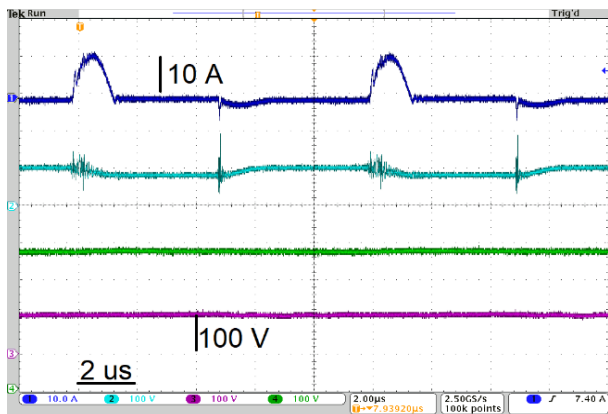


Fig. 12. Experimental waveforms of the IGBT transistor current, capacitor voltage, input and output voltage. CH1 -  $T_1$  high-side transistor drain current, CH2 - resonant capacitor voltage, CH3 - input voltage and CH4 - output voltage of the CESCVM.

From the waveforms presented in Fig. 13 it follows that in comparison to the SiC-based CESCVM (Fig. 8/ Fig. 10), waveforms of currents have better quality. Due to lower resistance in the circuits, the waveform of the current pulses has lower distortion from the sinusoidal function. Furthermore, less amount of disturbances are visible due to

lower parasitic capacitances. The IGBT based converter generates lower noise. The results of the laboratory efficiency measurements (Fig 13.) have confirmed that the CESCVM with IGBTs has worse efficiency than the SiC-based converter. The peak efficiency is 88,44%, which is nearly 2% below the peak efficiency achieved in the SiC-based converter. In the assumed range of power, IGBT-based design is less favorable even with better airflow during experiments. However, the performed tests with IGBT switches demonstrate the feasibility of such a design approach, which can be selected for converters with bigger power of load.

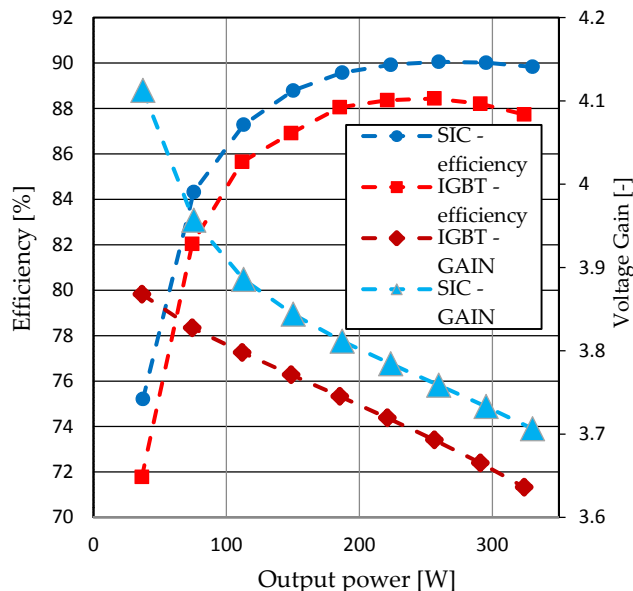


Fig. 13. Voltage gain and efficiency of the CESCVM with IGBTs and for switching frequency:  $f_s = 100$  kHz.

#### Temperature results of the power circuit

The infrared photography presented in Fig. 14. shows a large heat concentration near the T4 transistor (as was expected). The output capacitance discharge generates large energy losses of the transistor, which results in the significant heat generation. A picture presented in Fig. 14. has been recorded in a steady state after 30 minutes of CESCVM operation with 150 W of the load. It allows to observe the heat flow all over the surface of the power circuit.

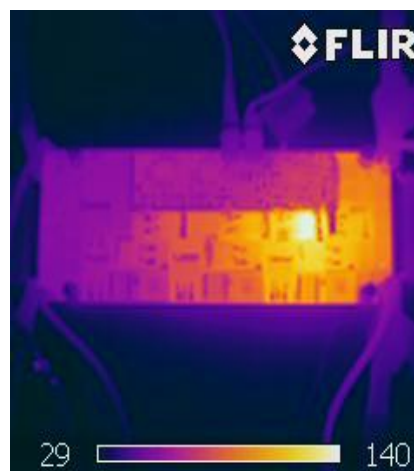


Fig. 14. Temperature distribution in the converter in a steady state operation. Visible thermal insulation, which is ensured by air-gap the PCB (Fig. 4). TC case temperature: 140°C.

According to the design assumption, thermally isolated gates driver (Fig. 4.) do not heat up from a power circuit. The charging capacitor heats the most due to greater stress and TC reliability reduces at higher operating temperatures.

The Tab. 2 consist of tests results in two different conditions. An important advantage of the converter is the invariance of parameters depending on the temperature. The CESCVM keeps constant its parameters such as efficiency and output voltage in two different temperatures.

Tab. 2. Power transfer efficiency and the voltage gain versus temperature. Switching frequency  $f_s = 150$  kHz and the input voltage  $U_{IN} = 100$  V.

Case temperature [°C]	110,0	150,0
Voltage gain [-]	3,86	3,85
Efficiency [%]	88,71	89,23

The typical circuit resistance changes by the temperature which affects the oscillation time. However, as the converter operates with a large time period between the charging and discharging stages it does not introduce a significant change to the operation of the converter. Based on the transistor datasheet [25], the turn-on losses ( $\Delta E_{ON}$ ) will decrease with the temperature rise which can improve the efficiency of the converter under high-temperature operation (Table 2). The temperature rise affects resistive components in the circuits, transistor losses as well as the forward voltages of diodes.

## Conclusions

The tested converter belongs to voltage multipliers family and the research results of the SiC-based CESCVM converter are presented in the paper. The converter has been tested in a configuration with air chokes. This is a prerequisite for the converter operation at high temperatures when the ferrite cores can reach the Curie temperature. The designed planar coil provided enough inductance for CESCVM. SiC transistors can operate using a simple and not expensive gateway driver system with top power supply switches based on the bootstrap circuit. A ceramic capacitor with an antiparallel Zener diode in the gate circuit allows to generate a negative voltage to switch off the transistors. The tested converter had high temperature rise of components and was tested at 25 deg of ambient. It is one of the possible case of the operating conditions. In case of higher ambient temperature the proposed test setup could achieve lower power or should operate with lower frequency. In future works, the design for operation with the temperature above 175 degrees Celsius should be analyzed. It requires the use of suitable switches, diodes, capacitors and PCB available in the market. Heat sink-less operation is the main advantage of the converter, which results in a smaller volume and weight of the power system.

All the results and conclusions presented in this paper are novel in comparison to the converter presented in literature where low voltage Si Mosfet switches were used.

It was assumed that the SiC-based CESCVM will allow for operation in high temperature, high switching frequency and high voltage stresses on switches. To confirm these assumptions efficiency of the converter has been precisely measured. Especially important results relate to the variation of efficiency versus temperature as well as the switching frequency.

The measured peak efficiency of SiC-based CESCVM is approximately 90% but the system allows to operate at high temperature (150°C) which makes it useful in some industrial applications. A temperature increase does not deteriorate CESCVM operation. Furthermore, the efficiency increases with working temperature rise.

A shape of efficiency versus Pout characteristic is very favorable in the tested case of SiC-based CESCVM (in comparison to Si Mosfet-based design presented in [16]) because the efficiency drop is not significant for bigger power.

The SiC -based converter was tested with two times higher voltage than in the case presented in [16] with comparable efficiency. It leads to the conclusion that Coss losses, associated with the voltage stress and the output capacitance of a transistor, are on the acceptable level. The switching losses do not increase significantly versus the switching frequency rise.

The results and comparison of efficiency characteristics in the IGBT-based CESCVM is a novel aspect as well. The results show that the application of suitable IGBT switch in CESCVM gives better quality of waveforms with lower noise. It can be important for the design of the converter. Nonsignificant worse efficiency results in comparison to SiC-based converter with the same temperature and the power range of operation was measured. However, the CESCVM designed for a bigger power IGBT-based approach can be more favorable than SiC or Mosfet -based, comparing operation quality, switching and conduction losses.

**Authors:** Mgr inż. Maciej Chojowski, Department of Power Electronics and Energy Control Systems, Faculty of Electrical Engineering, Automatics, Computer Science and Biomedical Engineering, AGH University of Science and Technology, 30-059 Krakow, Poland; E-mail: [chojo@agh.edu.pl](mailto:chojo@agh.edu.pl)

Dr hab. inż. Robert Stala, Department of Power Electronics and Energy Control Systems, Faculty of Electrical Engineering, Automatics, Computer Science and Biomedical Engineering, AGH University of Science and Technology, 30-059 Krakow, Poland; E-mail: [stala@agh.edu.pl](mailto:stala@agh.edu.pl)

Dr inż. Andrzej Mondzik, Department of Power Electronics and Energy Control Systems, Faculty of Electrical Engineering, Automatics, Computer Science and Biomedical Engineering, AGH University of Science and Technology, 30-059 Krakow, Poland; E-mail: [mondzik@agh.edu.pl](mailto:mondzik@agh.edu.pl)

Dr hab. inż. Adam Penczek, Department of Power Electronics and Energy Control Systems, Faculty of Electrical Engineering, Automatics, Computer Science and Biomedical Engineering, AGH University of Science and Technology, 30-059 Krakow, Poland; E-mail: [penczek@agh.edu.pl](mailto:penczek@agh.edu.pl)

## REFERENCES

- [1] Guo, X.; Xun, Q.; Li, Z.; Du, S. Silicon Carbide Converters and MEMS Devices for High-temperature Power Electronics: A Critical Review. *Micromachines* (Basel). 2019;10(6):406. Published 2019 Jun 19. doi:10.3390/mi10060406
- [2] Buttay, C.; Planson, D.; Allard, B.; Bergogne, D.; Bevilacqua, P.; Joubert, C.; Lazar, M.; Martin, C.; Morel, H.; Tournier, D.; Raynaud, C.; State of the art of high temperature power electronics, *Materials Science and Engineering: B*, Volume 176, Issue 4, 2011, Pages 283-288, ISSN 0921-5107.
- [3] Wang, Z. et al. Temperature-Dependent Short-Circuit Capability of Silicon Carbide Power MOSFETs, in *IEEE Transactions on Power Electronics*, vol. 31, no. 2, pp. 1555-1566, Feb. 2016. doi: 10.1109/TPEL.2015.2416358
- [4] Deshpande, A.; and Luo, F. Practical Design Considerations for a Si IGBT + SiC MOSFET Hybrid Switch: Parasitic Interconnect Influences, Cost, and Current Ratio Optimization, in *IEEE Transactions on Power Electronics*, vol. 34, no. 1, pp. 724-737, Jan. 2019. doi: 10.1109/TPEL.2018.2827989
- [5] Zhong, X.; Wu, X.; Zhou, W.; Sheng, K. An All-SiC High-Frequency Boost DC-DC Converter Operating at 320 °C Junction Temperature, in *IEEE Transactions on Power Electronics*, vol. 29, no. 10, pp. 5091-5096, Oct. 2014. doi: 10.1109/TPEL.2014.2311800.
- [6] Qi, F.; Wang, M.; Xu, L. Investigation and Review of Challenges in a High-Temperature 30-kVA Three-Phase Inverter Using SiC MOSFETs, in *IEEE Transactions on Industry Applications*, vol. 54, no. 3, pp. 2483-2491, May-June 2018. doi: 10.1109/TIA.2018.2796059

- [7] Olejniczak, K. et al., A compact 110 kVA, 140°C ambient, 105°C liquid cooled, all-SiC inverter for electric vehicle traction drives, 2017 IEEE Applied Power Electronics Conference and Exposition (APEC), Tampa, FL, 2017, pp. 735-742. doi: 10.1109/APEC.2017.7930776
- [8] Wrzecionko, B.; Bortis, D.; Kolar, J. W. A 120 °C Ambient Temperature Forced Air-Cooled Normally-off SiC JFET Automotive Inverter System, in IEEE Transactions on Power Electronics, vol. 29, no. 5, pp. 2345-2358, May 2014. doi: 10.1109/TPEL.2013.2294906
- [9] Juanjuan, L.; Zhe Z.; Jianhong, H.; Yi, H.; Hao, Z.; Ruixiang, H. High-temperature characteristics of SiC module and 100 kW SiC AC-DC converter at a junction temperature of 180 °C, Global Energy Interconnection, Volume 2, Issue 6, 2019, Pages 521-530,
- [10] Marzoughi, A.; Wang, J.; Burgos, R.; Boroyevich, D. Characterization and Evaluation of the State-of-the-Art 3.3-kV 400-A SiC MOSFETs, in IEEE Transactions on Industrial Electronics, vol. 64, no. 10, pp. 8247-8257, Oct. 2017.
- [11] Barlow, M.; et al. SiC-CMOS digital circuits for high temperature power conversion, 2016 IEEE 4th Workshop on Wide Bandgap Power Devices and Applications (WIPDA), Fayetteville, AR, 2016, pp. 223-227. doi: 10.1109/WIPDA.2016.7799942.
- [12] Lei, Y.; Pilawa-Podgurski, R.C.N. A general method for analyzing resonant and soft-charging Operation of switched-capacitor converters, IEEE Trans. Power Electron., vol. 30, no. 10, pp. 5650-5664, Oct. 2015.
- [13] Stala, R.; Piróg, S.; Penczek, A.; Kawa, A.; Waradzyn, Z.; Mondzik, A.; Skala, A. A family of high-power multilevel switched capacitor-based resonant DC-DC converters – operational parameters and novel concepts of topologies, , 65, No 5 pp. 639-651, 2017.
- [14] Waradzyn, Z.; Stala, R.; Mondzik, A.; Penczek, A.; Skala, A.; Pirog, S. Efficiency Analysis of MOSFET-Based Air-Choke Resonant DC-DC Step-Up Switched-Capacitor Voltage Multipliers. IEEE Transactions on Industrial Electronics, 64(11), pp. 8728–8738. doi: 10.1109/TIE.2017.2698368.
- [15] Waradzyn, Z.; Stala, R.; Mondzik, A.; Pirog, S. Switched capacitor-based power electronic converter – optimization of high frequency resonant circuit components. In: J. Kabziński, ed., Advanced Control of Electrical Drives and Power Electronic Converters, ser. Studies in Systems, Decision and Control, Vol. 75, Switzerland: Springer International Publishing AG, pp. 361–378.
- [16] Waradzyn, Z.; Stala, R.; Skala, A.; Mondzik, A.; and Penczek, A. A Cost-Effective Resonant Switched-Capacitor DC-DC Boost Converter – Experimental Results and Feasibility Model. Power Electronics and Drives 3(38), No. 1, 2018 DOI: 10.2478/pead-2018-0004.
- [17] Ye, Y.; Cheng K. W. E. A family of single-stage switched-capacitor– inductor PWM converters, IEEE Trans. Power Electron., vol. 28, no. 11, pp. 5196–5205, Nov. 2013, doi: 10.1109/TPEL.2013.2245918.
- [18] Wu, B.; Li, S.; Smedley, K. M.; and Singer, S. A family of two-switch boosting switched-capacitor converters, IEEE Trans. Power Electron., vol. 30, no. 10, pp. 5413–5424, Oct. 2015, doi: 10.1109/TPEL.2014.2375311.
- [19] Cao and Peng F. Z. A family of zero current switching switched-capacitor dc-dc converters, in Proc. 25th Annu. IEEE Appl. Power Electron. Conf. Expo., Feb. 21–25, 2010, pp. 1365–1372, doi: 10.1109/APEC.2010.5433407.
- [20] Jiao, Y.; Luo, F. L. N-switched-capacitor buck converter: topologies and analysis, IET Power Electron., vol. 4, no. 3, pp. 332–341, Mar. 2011, doi: 10.1049/iet-pel.2010.0104.
- [21] SH260 - High Performance, Polyimide Laminate and Prepreg. Online: <http://www.syst.com.cn>.
- [22] Mn-Zn Ferrite Material characteristics - November 2019 Online: [https://product.tdk.com/info/en/catalog/datasheets/ferrite\\_mn-zn\\_material\\_characteristics\\_en.pdf](https://product.tdk.com/info/en/catalog/datasheets/ferrite_mn-zn_material_characteristics_en.pdf)
- [23] Konrad, J.; Koini, M.; Schossmann, M.; Puff, M. New demands on DC link power capacitors, Congress on Automotive Electronic Systems - 3rd and 4th, December 2014
- [24] Surface Mount Multilayer Ceramic Chip Capacitors (SMD MLCCs) KC-LINK™ for Fast Switching Semiconductor Applications DC Link, Snubber, Resonator Capacitor, 150°C (Commercial & Automotive Grade) Online: [https://content.kemet.com/datasheets/KEM\\_C1039\\_KC-LINK\\_C0G.pdf](https://content.kemet.com/datasheets/KEM_C1039_KC-LINK_C0G.pdf)
- [25] Datasheet of UJ3C065030B3- 650V-27mW SiC FET. Preliminary, December 2019. Online: [https://unitedsic.com/datasheets/DS\\_UJ3C065030B3.pdf](https://unitedsic.com/datasheets/DS_UJ3C065030B3.pdf)
- [26] Datasheet of IKB15N65EH5 TRENCHSTOP™ 5 high speed switching IGBT copacked with full rated current RAPID 1 anti-parallel diode. Online: [https://www.infineon.com/dgdl/Infineon- IKB15N65EH5-DS-v02\\_01- EN.pdf?fileId=5546d46262b31d2e0162cd1328dc4914](https://www.infineon.com/dgdl/Infineon- IKB15N65EH5-DS-v02_01- EN.pdf?fileId=5546d46262b31d2e0162cd1328dc4914)
- [27] The datasheet of UCC21520, UCC21520A 4-A, 6-A, 5.7-kVRMS Isolated Dual-Channel Gate Driver datasheet (Rev. C): <http://www.ti.com/lit/ds/symlink/ucc21520.pdf>
- [28] Timothy Hegarty, An overview of conducted EMI specifications for power supplies, Texas Instruments, 2018. Online: [https://www.ti.com/lit/wp/slyy136/slyy136.pdf?ts=1595574171360&ref\\_url=https%253A%252F%252Fwww.google.com%252F](https://www.ti.com/lit/wp/slyy136/slyy136.pdf?ts=1595574171360&ref_url=https%253A%252F%252Fwww.google.com%252F)